Publishing House
AKAPIT

COMPUTER METHODS IN MATERIALS SCIENCE

Informatyka w Technologii Materiałów

Vol. 9, 2009, No. 1

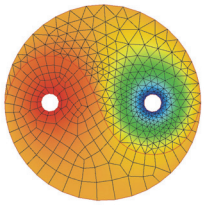

INTERACTION OF PENNY-SHAPED CRACK AND SPHERICAL INCLUSION IN 3D PARTICULATE ELASTIC COMPOSITE: BIEM CALCULATION OF MODE-I DYNAMIC STRESS INTENSITY FACTOR

OKSANA KHAY[1], VIKTOR MYKHAS'KIV[1], JAN SLADEK[2], VLADIMIR SLADEK[2], CHUANZENG ZHANG[3]

[1] Pidstryhach Institute for Applied Problems of Mechanics and Mathematics NASU,
3-b Naukova Str., 79060 Lviv, Ukraine
[2] Department of Mechanics, Institute of Construction and Architecture,
9 Dubravska Cesta, 84503 Bratislava, Slovakia
[3] Department of Civil Engineering, University of Siegen,
9-11 Paul-Bonatz-Str., 57076 Siegen, Germany

Abstract

The interaction between a penny-shaped crack and a spherical elastic inclusion embedded in an infinite elastic matrix subjected to a time-harmonic crack-face loading is investigated. Boundary integral equations (BIEs) are applied for the numerical solution of the problem in the frequency domain. The singularity subtraction and the mapping techniques in conjunction with a collocation scheme are implemented for the regularization and the discretization of the BIEs by taking into account the local structure of the solution at the crack front. As a numerical example, a crack under tensile loading of constant amplitude, where the center of the interacting particle lies in the crack plane, is considered. The reinforcing properties of the inclusion are revealed by the mode-I dynamic stress intensity factor (SIF) as a function of angular coordinate of the crack front for different frequencies and material combinations of the matrix and the inclusion.

Key words: 3D particulate composite, matrix penny-shaped crack, spherical elastic inclusion, time-harmonic loading, dynamic stress intensity factor, boundary integral equations method

1. INTRODUCTION

To understand the role of volumetric inclusions as shielding or amplification objects in advanced particle- or fiber-reinforced composites under elastic wave loading conditions, their interaction with the defects like cracks subjected to dynamic loading should be investigated. The boundary integral equations method (BIEM) is ideally suited for such kind of analyses for three-dimensional (3D) problems, which is shown in the static analysis for the interaction of a penny-shaped crack with a spherical elastic inclusion in an infinite elastic matrix [3,6,8]. The single crack [1,7,9] and the single inclusion [4,5] problems under a dynamic load were considered by the BIEM too. However, the interaction of a spherical elastic inclusion and a matrix penny-shaped crack under dynamic loading has not been investigated according to the author's knowledge.

In this paper, the BIEM is presented to analyze the influence of a spherical elastic inclusion on the dynamic stress intensity factor of a neighboring penny-shaped crack. The interacting objects are located in a 3D infinite elastic matrix and the crack faces are subjected to a time-harmonic loading. For the sake of brevity, the symmetric problem with respect to the crack plane is considered. The system

ISSN 1641-8581

of six coupled displacement BIEs and one traction BIE for the interfacial displacements and tractions as well as the normal crack-opening-displacement (COD) are deduced by satisfying the perfect contact conditions on the matrix-inclusion interface and the stress conditions on the crack surfaces. They are solved numerically after their regularization by the integral operators with elastostatic kernels and the discretization by the collocation scheme. The local behavior of the COD near the crack front is taken into account implicitly in the numerical method, which allows for a direct and accurate computation of the mode-I dynamic SIF. Numerical calculations are carried out for an inclusion and a crack with the same diameter under a tensile crack surface loading of constant amplitude. The effects of the frequency and the materials combination of the matrix-inclusion on the distribution of the mode-I dynamic SIF along the crack front are investigated.

2. BOUNDARY INTEGRAL FORMULATION AND NUMERICAL SOLUTION OF THE PROBLEM

Consider an infinite isotropic elastic matrix with a penny-shaped crack of radius a^C and an isotropic elastic spherical inclusion of radius a^I with its center O^I located at the crack plane $x_3 = 0$ and a distance d from the crack center O^C. The matrix material is specified by the mass density ρ^M, the shear modulus G^M and Poisson's ratio ν^M, while the inclusion material is characterized by ρ^I, G^I, and ν^I, respectively. A perfect contact between the matrix and the inclusion is assumed, which implies that the displacements and the stresses are continuous across the matrix - inclusion surface S^I. The crack surfaces occupying the domain S^C are subjected to a tensile time-harmonic loading with the circular frequency ω and the amplitude $\mathbf{N}^+ = -\mathbf{N}^- = \mathbf{N}(0,0,N_3)$ (figure 1). For simplicity, the common factor $\exp(-i\omega t)$ is suppressed throughout the analysis.

In accordance to the superposition principle the displacement field $\mathbf{u}^M\left(u_1^M, u_2^M, u_3^M\right)$ in the matrix can be written as

$$\mathbf{u}^M = \mathbf{u}^S + \mathbf{u}^C, \qquad (1)$$

where the terms $\mathbf{u}^S\left(u_1^S, u_2^S, u_3^S\right)$ and $\mathbf{u}^C\left(u_1^C, u_2^C, u_3^C\right)$ describe the contributions to the total wave field scattered by the inclusion and induced by the crack, respectively, which can be represented by the following boundary integrals [2, 9]:

$$u_j^S(\mathbf{x}) = \iint_{S^I}\left[T_{jk}^M\left(\mathbf{x},\mathbf{y},\mathbf{n}^I\right)u_k^M(\mathbf{y}) - U_{jk}^M(\mathbf{x},\mathbf{y})t_k^M(\mathbf{y})\right]dS_{\mathbf{y}},$$

$$u_j^C(\mathbf{x}) = \iint_{S^C} T_{j3}^M\left(\mathbf{x},\mathbf{y},\mathbf{n}^C\right)\Delta u(\mathbf{y})\,dS_{\mathbf{y}}. \qquad (2)$$

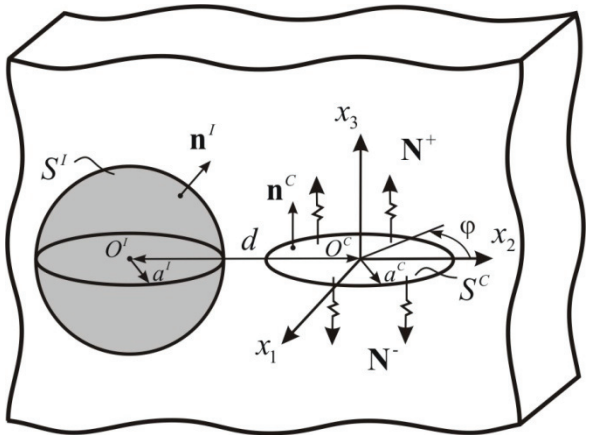

Fig. 1. *Problem geometry.*

Hereafter all indices range from 1 to 3 and repeated indices imply summation, $\mathbf{t}^M\left(t_1^M, t_2^M, t_3^M\right)$ is the traction vector caused by the influence of the inclusion on the matrix, $\Delta u(\mathbf{x}) = u_3^M(x_1, x_2, +0) - u_3^M(x_1, x_2, -0)$ is the normal COD (due to the symmetry of the problem the tangential CODs are equal to zero), $\mathbf{n}^I(n_1^I, n_2^I, n_3^I)$ is the unit vector normal to the inclusion surface as depicted in figure 1, $\mathbf{n}^C(0,0,1)$ is the normal vector to the crack surface, U_{ij}^M and T_{ij}^M are the time-harmonic displacement and traction fundamental solutions, namely

$$U_{jk}^M(\mathbf{x},\mathbf{y}) = \frac{1}{4\pi G^M \omega_{2M}^2}\left[f_1\left(|\mathbf{x}-\mathbf{y}|\right)\delta_{jk} - f_2\left(|\mathbf{x}-\mathbf{y}|\right)\frac{(x_j - y_j)(x_k - y_k)}{|\mathbf{x}-\mathbf{y}|^2}\right],$$

$$T_{jk}^{M}(\mathbf{x},\mathbf{y},\mathbf{n})=\frac{1}{4\pi\omega_{2M}^{2}}\left\langle\left\{\left[g_2\left(|\mathbf{x}-\mathbf{y}|\right)+g_1\left(|\mathbf{x}-\mathbf{y}|\right)\right]\delta_{jk}+\right.\right.$$

$$2\left[g_3\left(|\mathbf{x}-\mathbf{y}|\right)-2g_2\left(|\mathbf{x}-\mathbf{y}|\right)\right]\times$$

$$\left.\frac{(x_j-y_j)(x_k-y_k)}{|\mathbf{x}-\mathbf{y}|^2}\right\}\frac{(x_m-y_m)}{|\mathbf{x}-\mathbf{y}|}n_m(\mathbf{y})+$$

$$\frac{2}{1-2\nu^M}\left\{\nu^M\left[g_1\left(|\mathbf{x}-\mathbf{y}|\right)-g_3\left(|\mathbf{x}-\mathbf{y}|\right)\right]+\right.$$

$$\left.+g_2\left(|\mathbf{x}-\mathbf{y}|\right)\right\}\frac{(x_j-y_j)}{|\mathbf{x}-\mathbf{y}|}n_k(\mathbf{y})+$$

$$\left.\left[g_2\left(|\mathbf{x}-\mathbf{y}|\right)+g_1\left(|\mathbf{x}-\mathbf{y}|\right)\right]\frac{(x_k-y_k)}{|\mathbf{x}-\mathbf{y}|}n_j(\mathbf{y})\right\rangle. \quad (3)$$

In equations (3)

$$f_1(r)=\left[\left(1-i\omega_{1M}r\right)\exp(i\omega_{1M}r)-\right.$$
$$\left.\left(1-i\omega_{2M}r-\omega_{2M}^2r^2\right)\exp(i\omega_{2M}r)\right]r^{-3},$$

$$f_2(r)=\left[\left(3-3i\omega_{1M}r-\omega_{1M}^2r^2\right)\exp(i\omega_{1M}r)-\right.$$
$$\left.\left(3-3i\omega_{2M}r-\omega_{2M}^2r^2\right)\exp(i\omega_{2M}r)\right]r^{-3},$$

$$g_1(r)=\left[\left(3-3i\omega_{1M}r-\omega_{1M}^2r^2\right)\exp(i\omega_{1M}r)-\right.$$
$$\left.\left(3-3i\omega_{2M}r-2\omega_{2M}^2r^2+i\omega_{2M}^3r^3\right)\exp(i\omega_{2M}r)\right]r^{-4},$$

$$g_2(r)=\left[\left(3-3i\omega_{1M}r-\omega_{1M}^2r^2\right)\exp(i\omega_{1M}r)-\right.$$
$$\left.\left(3-3i\omega_{2M}r-\omega_{2M}^2r^2\right)\exp(i\omega_{2M}r)\right]r^{-4},$$

$$g_3(r)=\left[\left(9-9i\omega_{1M}r-4\omega_{1M}^2r^2+i\omega_{1M}^3r^3\right)\exp(i\omega_{1M}r)\right.$$
$$\left.-\left(9-9i\omega_{2M}r-4\omega_{2M}^2r^2+i\omega_{2M}^3r^3\right)\exp(i\omega_{2M}r)\right]r^{-4}, \quad (4)$$

δ_{jk} is the Kronecker symbol, $\omega_{jM}=\omega/c_j^M$ $(j=1,2)$ are the wave numbers of the matrix, $c_2^M=\sqrt{G^M/\rho^M}$ and $c_1^M=c_2^M\sqrt{2\left(1-\nu^M\right)/\left(1-2\nu^M\right)}$ are the transverse and the longitudinal wave velocities of the matrix.

From equations (1) and (2) we can obtain the following integral representations for the stress components σ_{jm}^M in the matrix

$$\sigma_{jm}^M(\mathbf{x})=\iint_{S^I}\left[D_{jmk}^M\left(\mathbf{x},\mathbf{y},\mathbf{n}^I\right)u_k^M(\mathbf{y})-\right.$$
$$\left.S_{jmk}^M(\mathbf{x},\mathbf{y})t_k^M(\mathbf{y})\right]dS_{\mathbf{y}}+\iint_{S^C}D_{jm3}^M\left(\mathbf{x},\mathbf{y},\mathbf{n}^C\right)\Delta u(\mathbf{y})dS_{\mathbf{y}}. \quad (5)$$

Here S_{jmk}^M and D_{jmk}^M can be derived by the differentiation of U_{jk}^M and T_{jk}^M with respect to $\mathbf{x}$ and the application of the stress-strain relationship, whose explicit expressions can be found in [1]. It should be mentioned that the exterior wave fields (1), (2) and (5) satisfy the radiation conditions at infinity.

The interior displacement field $\mathbf{u}^I\left(u_1^I,u_2^I,u_3^I\right)$ in the inclusion can be expressed by the following representation

$$u_j^I(\mathbf{x})=\iint_{S^I}\left[U_{jk}^I(\mathbf{x},\mathbf{y})t_k^I(\mathbf{y})-\right.$$
$$\left.T_{jk}^I\left(\mathbf{x},\mathbf{y},\mathbf{n}^I\right)u_k^I(\mathbf{y})\right]dS_{\mathbf{y}}, \quad (6)$$

in which $\mathbf{t}^I\left(t_1^I,t_2^I,t_3^I\right)$ is the traction vector caused by the influence of the matrix on the inclusion, U_{jk}^I and T_{jk}^I can be obtained from equations (3) and (4) by replacing the material constants ρ^M, G^M and ν^M with ρ^I, G^I and ν^I, respectively.

Considering the continuity conditions $\mathbf{u}^M\left(u_1^M,u_2^M,u_3^M\right)=\mathbf{u}^I\left(u_1^I,u_2^I,u_3^I\right)=\mathbf{u}\left(u_1,u_2,u_3\right)$, $\mathbf{t}^M\left(t_1^M,t_2^M,t_3^M\right)=\mathbf{t}^I\left(t_1^I,t_2^I,t_3^I\right)=\mathbf{t}\left(t_1,t_2,t_3\right)$ on $\mathbf{x}\in S^I$ in the representations (1), (2) and (6) and substituting equation (5) into the boundary condition $\sigma_{33}^M=-N_3$ on $\mathbf{x}\in S^C$, a system of seven coupled BIEs for the interfacial quantities u_j, t_j $(j=1,2,3)$ and the COD Δu is obtained as

$$\frac{1}{2}u_j(\mathbf{x})-\iint_{S^I}T_{jk}^M\left(\mathbf{x},\mathbf{y},\mathbf{n}^I\right)u_k(\mathbf{y})dS_{\mathbf{y}}+$$
$$\iint_{S^I}U_{jk}^M(\mathbf{x},\mathbf{y})t_k(\mathbf{y})dS_{\mathbf{y}}-$$
$$-\iint_{S^C}T_{j3}^M\left(\mathbf{x},\mathbf{y},\mathbf{n}^C\right)\Delta u(\mathbf{y})dS_{\mathbf{y}}=0,\quad \mathbf{x}\in S^I,$$

$$\frac{1}{2}u_j(\mathbf{x})+\iint_{S^I} T^I_{jk}(\mathbf{x},\mathbf{y},\mathbf{n}^I)u_k(\mathbf{y})dS_{\mathbf{y}} - \iint_{S^I} U^I_{jk}(\mathbf{x},\mathbf{y})t_k(\mathbf{y})dS_{\mathbf{y}} = 0, \quad \mathbf{x}\in S^I,$$

$$\iint_{S^I} D^M_{33k}(\mathbf{x},\mathbf{y},\mathbf{n}^I)u_k(\mathbf{y})dS_{\mathbf{y}} - \iint_{S^I} S^M_{33k}(\mathbf{x},\mathbf{y})t_k(\mathbf{y})dS_{\mathbf{y}} + \iint_{S^C} D^M_{333}(\mathbf{x},\mathbf{y},\mathbf{n}^C)\Delta u(\mathbf{y})dS_{\mathbf{y}} = -N_3(\mathbf{x}), \quad \mathbf{x}\in S^C. \tag{7}$$

It should be remarked here that the BIEs (7) contain hypersingular kernel D^M_{333}, strongly singular kernels T^M_{jk}, T^I_{jk}, and weakly singular kernels U^M_{jk}, U^I_{jk}, which require special attention in the numerical solution procedure. For the additive isolation of the singularities, the BIEs (7) are rewritten as

$$\frac{1}{2}u_j(\mathbf{x})-\iint_{S^I}\tilde{T}^M_{jk}(\mathbf{x},\mathbf{y},\mathbf{n}^I)u_k(\mathbf{y})dS_{\mathbf{y}} + \iint_{S^I}\tilde{U}^M_{jk}(\mathbf{x},\mathbf{y})t_k(\mathbf{y})dS_{\mathbf{y}} - \iint_{S^I}\left[T^M_{jk}(\mathbf{x},\mathbf{y},\mathbf{n}^I)-\tilde{T}^M_{jk}(\mathbf{x},\mathbf{y},\mathbf{n}^I)\right]u_k(\mathbf{y})dS_{\mathbf{y}} + \iint_{S^I}\left[U^M_{jk}(\mathbf{x},\mathbf{y})-\tilde{U}^M_{jk}(\mathbf{x},\mathbf{y})\right]t_k(\mathbf{y})dS_{\mathbf{y}} - \iint_{S^C}T^M_{j3}(\mathbf{x},\mathbf{y},\mathbf{n}^C)\Delta u(\mathbf{y})dS_{\mathbf{y}} = 0, \quad \mathbf{x}\in S^I,$$

$$\frac{1}{2}u_j(\mathbf{x})+\iint_{S^I}\tilde{T}^I_{jk}(\mathbf{x},\mathbf{y},\mathbf{n}^I)u_k(\mathbf{y})dS_{\mathbf{y}} - \iint_{S^I}\tilde{U}^I_{jk}(\mathbf{x},\mathbf{y})t_k(\mathbf{y})dS_{\mathbf{y}} + \iint_{S^I}\left[T^I_{jk}(\mathbf{x},\mathbf{y},\mathbf{n}^I)-\tilde{T}^I_{jk}(\mathbf{x},\mathbf{y},\mathbf{n}^I)\right]u_k(\mathbf{y})dS_{\mathbf{y}} - \iint_{S^I}\left[U^I_{jk}(\mathbf{x},\mathbf{y})-\tilde{U}^I_{jk}(\mathbf{x},\mathbf{y})\right]t_k(\mathbf{y})dS_{\mathbf{y}} = 0, \quad \mathbf{x}\in S^I,$$

$$\iint_{S^C}\tilde{D}^M_{333}(\mathbf{x},\mathbf{y},\mathbf{n}^C)\Delta u(\mathbf{y})dS_{\mathbf{y}} + \iint_{S^C}\hat{D}^M_{333}(\mathbf{x},\mathbf{y},\mathbf{n}^C)\Delta u(\mathbf{y})dS_{\mathbf{y}} + \iint_{S^C}\left[D^M_{333}(\mathbf{x},\mathbf{y},\mathbf{n}^C)-\tilde{D}^M_{333}(\mathbf{x},\mathbf{y},\mathbf{n}^C)-\hat{D}^M_{333}(\mathbf{x},\mathbf{y},\mathbf{n}^C)\right]\Delta u(\mathbf{y})dS_{\mathbf{y}} + \iint_{S^I}D^M_{33k}(\mathbf{x},\mathbf{y},\mathbf{n}^I)u_k(\mathbf{y})dS_{\mathbf{y}} - \iint_{S^I}S^M_{33k}(\mathbf{x},\mathbf{y})t_k(\mathbf{y})dS_{\mathbf{y}} = -N_3(\mathbf{x}), \quad \mathbf{x}\in S^C. \tag{8}$$

Here $\tilde{U}^L_{jk}$, $\tilde{T}^L_{jk}$ $(L=M,I)$ and $\tilde{D}^M_{333}$ are the static counterparts of the kernels U^L_{jk}, T^L_{jk} $(L=M,I)$ and D^M_{333}, while $\hat{D}^M_{333}$ is the weakly singular part of D^M_{333}, i.e.,

$$\tilde{U}^L_{jk}(\mathbf{x},\mathbf{y}) = \frac{1}{16\pi G^L(1-\nu^L)|\mathbf{x}-\mathbf{y}|}\left[(3-4\nu^L)\delta_{jk}+\frac{(x_j-y_j)(x_k-y_k)}{|\mathbf{x}-\mathbf{y}|^2}\right],$$

$$\tilde{T}^L_{jk}(\mathbf{x},\mathbf{y},\mathbf{n}) = \frac{1}{8\pi(1-\nu^L)|\mathbf{x}-\mathbf{y}|^2}\left\{\left[(1-2\nu^L)\delta_{jk}+3\frac{(x_j-y_j)(x_k-y_k)}{|\mathbf{x}-\mathbf{y}|^2}\right]\frac{(x_m-y_m)}{|\mathbf{x}-\mathbf{y}|}n_m(\mathbf{y}) - (1-2\nu^L)\left[\frac{(x_j-y_j)}{|\mathbf{x}-\mathbf{y}|}n_k(\mathbf{y})-\frac{(x_k-y_k)}{|\mathbf{x}-\mathbf{y}|}n_j(\mathbf{y})\right]\right\},$$

$$\tilde{D}^M_{333}(\mathbf{x},\mathbf{y}) = \frac{G^M}{4\pi(1-\nu^M)|\mathbf{x}-\mathbf{y}|^3},$$

$$\hat{D}^M_{333}(\mathbf{x},\mathbf{y}) = \frac{(7-12\nu^M+8(\nu^M)^2)\omega^2_{2M}G^M}{32\pi(1-\nu^M)^2|\mathbf{x}-\mathbf{y}|}. \tag{9}$$

The expressions in the square brackets in equations (8) are regular at $|\mathbf{x}-\mathbf{y}|\to 0$. The advantage of the rewritten equations (8) in comparison with equations (7) is that the singular kernels in equations (8) become real and have the elastostatic form.

For the regularization of the first six equations of the system (8) the solution for the rigid body can be used [2]. Then the weakly singular forms of these equations are obtained as

$$u_j(\mathbf{x})-\iint_{S^I}\tilde{T}^M_{jk}(\mathbf{x},\mathbf{y},\mathbf{n}^I)\left[u_k(\mathbf{y})-u_k(\mathbf{x})\right]dS_{\mathbf{y}} +$$

$$\iint_{S^I} \tilde{U}^M_{jk}(\mathbf{x},\mathbf{y}) t_k(\mathbf{y})\, dS_{\mathbf{y}} -$$

$$\iint_{S^I} \left[T^M_{jk}(\mathbf{x},\mathbf{y},\mathbf{n}^I) - \tilde{T}^M_{jk}(\mathbf{x},\mathbf{y},\mathbf{n}^I) \right] u_k(\mathbf{y})\, dS_{\mathbf{y}} +$$

$$\iint_{S^I} \left[U^M_{jk}(\mathbf{x},\mathbf{y}) - \tilde{U}^M_{jk}(\mathbf{x},\mathbf{y}) \right] t_k(\mathbf{y})\, dS_{\mathbf{y}} -$$

$$\iint_{S^C} T^M_{j3}(\mathbf{x},\mathbf{y},\mathbf{n}^C) \Delta u(\mathbf{y})\, dS_{\mathbf{y}} = 0, \qquad \mathbf{x} \in S^I,$$

$$\iint_{S^I} \tilde{T}^I_{jk}(\mathbf{x},\mathbf{y},\mathbf{n}^I) \left[u_k(\mathbf{y}) - u_k(\mathbf{x}) \right] dS_{\mathbf{y}} -$$

$$\iint_{S^I} \tilde{U}^I_{jk}(\mathbf{x},\mathbf{y}) t_k(\mathbf{y})\, dS_{\mathbf{y}} + \iint_{S^I} \left[T^I_{jk}(\mathbf{x},\mathbf{y},\mathbf{n}^I) - \right.$$

$$\left. \tilde{T}^I_{jk}(\mathbf{x},\mathbf{y},\mathbf{n}^I) \right] u_k(\mathbf{y})\, dS_{\mathbf{y}} -$$

$$\iint_{S^I} \left[U^I_{jk}(\mathbf{x},\mathbf{y}) - \tilde{U}^I_{jk}(\mathbf{x},\mathbf{y}) \right] t_k(\mathbf{y})\, dS_{\mathbf{y}} = 0,$$

$$\mathbf{x} \in S^I, \qquad (10)$$

Regularization of the last equation of the system (8) considers the COD behavior at the crack front properly by using

$$\Delta u(\mathbf{x}) = \sqrt{(a^C)^2 - x_1^2 - x_2^2}\ \alpha(\mathbf{x}),$$

where $\alpha(\mathbf{x})$ is a new unknown function, and the analytical evaluation of singular integrals of the type

$$I^m_{jk}(\mathbf{x}) = \iint_{S^C} \frac{\sqrt{(a^C)^2 - y_1^2 - y_2^2}\,(y_1 - x_1)^j (y_2 - x_2)^k}{|\mathbf{x} - \mathbf{y}|^m} dS_{\mathbf{y}},$$

$$\mathbf{x} \in S^C. \qquad (11)$$

The singular integrals (11) can be computed analytically as

$$I^3_{00}(\mathbf{x}) = -\pi^2, \qquad I^1_{00}(\mathbf{x}) = \frac{\pi^2}{4}\left(2(a^C)^2 - x_1^2 - x_2^2\right),$$

$$I^3_{10}(\mathbf{x}) = -\frac{\pi^2}{2} x_1, \qquad I^3_{01}(\mathbf{x}) = -\frac{\pi^2}{2} x_2,$$

$$I^3_{20}(\mathbf{x}) = \frac{\pi^2}{16}\left(4(a^C)^2 - x_1^2 - 3x_2^2\right),$$

$$I^3_{02}(\mathbf{x}) = \frac{\pi^2}{16}\left(4(a^C)^2 - 3x_1^2 - x_2^2\right),$$

$$I^3_{11}(\mathbf{x}) = \frac{\pi^2}{8} x_1 x_2. \qquad (12)$$

Substitution of the integrals (12) into the last equation of the system (8) yields the regular version of this equation in the form

$$\frac{G^M}{4\pi(1-\nu^M)} \left\{ \left[I^3_{00}(\mathbf{x}) + \frac{(7 - 12\nu^M + 8(\nu^M)^2)}{8(1-\nu^M)} \omega^2_{2M} I^1_{00}(\mathbf{x}) \right] \right.$$

$$\left| \alpha(\mathbf{x}) + I^3_{10}(\mathbf{x}) \frac{\partial \alpha(\mathbf{x})}{\partial x_1} + I^3_{01}(\mathbf{x}) \frac{\partial \alpha(\mathbf{x})}{\partial x_2} + \right.$$

$$\left. \frac{1}{2} I^3_{20}(\mathbf{x}) \frac{\partial^2 \alpha(\mathbf{x})}{\partial x_1^2} + \frac{1}{2} I^3_{02}(\mathbf{x}) \frac{\partial^2 \alpha(\mathbf{x})}{\partial x_2^2} + I^3_{11}(\mathbf{x}) \frac{\partial^2 \alpha(\mathbf{x})}{\partial x_1 \partial x_2} \right\} +$$

$$\iint_{S^C} \sqrt{(a^C)^2 - y_1^2 - y_2^2}\ \tilde{D}^M_{333}(\mathbf{x},\mathbf{y},\mathbf{n}^C) \times$$

$$\times \left[\alpha(\mathbf{y}) - \alpha(\mathbf{x}) - (y_1 - x_1) \frac{\partial \alpha(\mathbf{x})}{\partial x_1} - (y_2 - x_2) \frac{\partial \alpha(\mathbf{x})}{\partial x_2} - \right.$$

$$\frac{1}{2}(y_1 - x_1)^2 \frac{\partial^2 \alpha(\mathbf{x})}{\partial x_1^2} - \frac{1}{2}(y_2 - x_2)^2 \frac{\partial^2 \alpha(\mathbf{x})}{\partial x_2^2} -$$

$$\left. \cdot (y_1 - x_1)(y_2 - x_2) \frac{\partial^2 \alpha(\mathbf{x})}{\partial x_1 \partial x_2} \right] dS_{\mathbf{y}} +$$

$$\iint_{S^C} \sqrt{(a^C)^2 - y_1^2 - y_2^2}\ \hat{D}^M_{333}(\mathbf{x},\mathbf{y},\mathbf{n}^C) \left[\alpha(\mathbf{y}) - \alpha(\mathbf{x}) \right] dS_{\mathbf{y}} +$$

$$\iint_{S^C} \sqrt{(a^C)^2 - y_1^2 - y_2^2} \left[D^M_{333}(\mathbf{x},\mathbf{y},\mathbf{n}^C) - \tilde{D}^M_{333}(\mathbf{x},\mathbf{y},\mathbf{n}^C) - \right.$$

$$\left. \cdot \hat{D}^M_{333}(\mathbf{x},\mathbf{y},\mathbf{n}^C) \right] \alpha(\mathbf{y})\, dS_{\mathbf{y}} +$$

$$\iint_{S^I} D^M_{33k}(\mathbf{x},\mathbf{y},\mathbf{n}^I) u_k(\mathbf{y})\, dS_{\mathbf{y}} -$$

$$\iint_{S^I} S^M_{33k}(\mathbf{x},\mathbf{y}) t_k(\mathbf{y})\, dS_{\mathbf{y}} = -N_3(\mathbf{x}), \qquad \mathbf{x} \in S^C. \qquad (13)$$

A system of linear algebraic equations is obtained by collocating the BIEs (10) at the nodal points of eight-nodes quadrilateral elements and six-nodes triangular elements near the poles of the inclusion surface, where the boundary element mesh is formed by a uniform division of the inclusion surface in the direction of polar coordinates φ and θ, and quadratic shape functions are applied for the parametrical description of the surface. To avoid the weakly singular peculiarity in these equations a variable change is used. For example, if the nodal and the source points coincide at the point $(-1,-1)$ of the local coordinate system $O\xi_1\xi_2$ with the origin at the center of a unit square subdivided into two trian-

gles, the linear transformation of the coordinates is given by

$$\xi_1 = \frac{1}{4}(1-\eta_2)(1+\eta_1) - \frac{1}{2}(1-\eta_1) + \frac{1}{4}(1+\eta_2)(1+\eta_1),$$

$$\xi_2 = \frac{1}{4}(1-\eta_2)(1+\eta_1) - \frac{1}{2}(1-\eta_1) - \frac{1}{4}(1+\eta_2)(1+\eta_1),$$

$$\{-1 \le \eta_1 \le 1, -1 \le \eta_2 \le 1\}. \qquad (14)$$

The discretization of the BIE (13) is realized by a collocation scheme, where the boundary element mesh is formed by a uniform division of the planar crack surface in the direction of the polar coordinates r and φ, and an additional circular element located at the centre of crack. In this analysis, linear approximation within each element is used for the interfacial quantities u_j and t_j, while constant approximation is adopted for the crack-domain function $\alpha(\mathbf{x})$. In the numerical calculations, the inclusion surface was divided into 144 elements and the crack surface was discretized into 161 elements.

3. NUMERICAL RESULTS

Numerical analysis is focused on the mode-I dynamic SIF K_{I}, which is related to α by

$$K_{\mathrm{I}}(\varphi) = \frac{G\sqrt{\pi a^C}}{2(1-\nu)}\alpha(\mathbf{x})\Big|_{\substack{x_1=a^C\cos\varphi;\\ x_2=a^C\sin\varphi,}} \qquad (15)$$

where φ is the angular coordinate of the crack front (figure 1).

As an example, interacting penny-shaped crack and spherical inclusion of the same radii $a^C = a^I = a$ are considered. The crack is subjected to a tensile loading of constant amplitude N_0. The mass densities and Poisson's ratios of the matrix and the inclusion are taken as equal, i.e., $\rho^M = \rho^I$ and $\nu^M = \nu^I = 0.25$, and the materials dissimilarity is provided by the different shear modulus with the ratio $G = G^I/G^M$. The static SIF $K_{\mathrm{I}}^* = 2N_0\sqrt{a/\pi}$ is chosen as a normalization factor for the dynamic SIF, so that $\bar{K}_{\mathrm{I}} = |K_{\mathrm{I}}|/K_{\mathrm{I}}^*$.

Since the problem for the considered crack-inclusion configuration is not axially symmetric with respect to the Ox_3-axis, the mode-I dynamic SIF changes from point to point around the crack front.

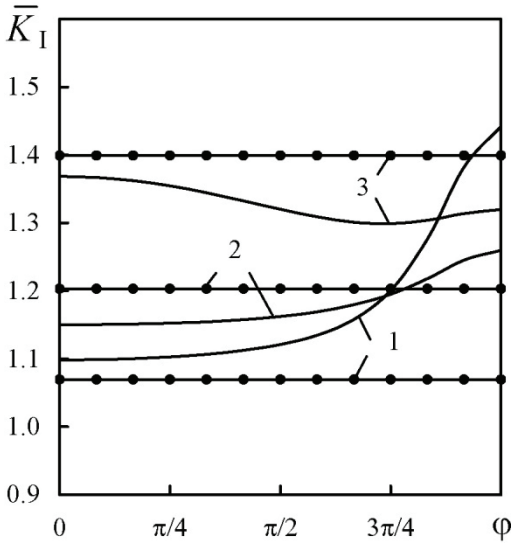

Fig. 2. Normalized amplitudes of the mode-I dynamic SIF along the crack front near a "soft" inclusion: $d = 3a$; $G = 0.2$; $1 - \omega_{1M}a = 0.3$; $2 - \omega_{1M}a = 0.5$; $3 - \omega_{1M}a = 0.7$; marked lines are for a single crack.

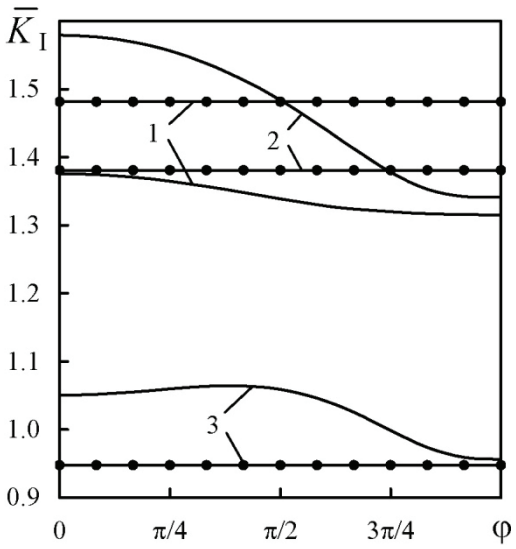

Fig. 3. Normalized amplitudes of the mode-I dynamic SIF along the crack front near a "hard" inclusion: $d = 2.5a$; $G = 5.0$; $1 - \omega_{1M}a = 0.8$; $2 - \omega_{1M}a = 1.0$; $3 - \omega_{1M}a = 1.2$; marked lines are for a single crack.

This fact is demonstrated in figures 2 and 3, where $\bar{K}_{\mathrm{I}}$ as a function of the angular coordinate φ of the crack front for different normalized wave numbers $\omega_{1M}a$ is presented. For the purpose of comparison, $\bar{K}_{\mathrm{I}}$ for a single crack is taken from [9] and shown by the marked lines. At low frequencies the interaction of a "soft" inclusion and a crack (figure 2) causes an increase of the mode-I SIF amplitudes in comparison with that for a single crack. In other words, such inclusion provides an amplification

effect for the crack. An opposite shielding tendency is observed for a „hard“ inclusion near a penny-shaped crack (figure 3). The dynamic overshoot (undershoot) in $\overline{K}_{\mathrm{I}}$ is mostly obvious at the crack front points nearest to the inclusion. With increasing frequency the $\overline{K}_{\mathrm{I}}$-factor can be either smaller or larger than that for a single crack depending on the position at the crack front. Furthermore, the role of a "soft" inclusion changes from amplification to shielding at a high wave number $\omega_{1M} a = 0.7$. Similarly, a „hard“ inclusion acts as an amplification object for the $\overline{K}_{\mathrm{I}}$-factor at $\omega_{1M} a = 1.2$.

ACKNOWLEDGEMENT

This work is supported by the INTAS (Project No. 05-1000008-7979).

REFERENCES

1. Ariza, M.P., Dominguez, J., 2002, General BE Approach for Three-Dimensional Dynamic Fracture Analysis, Eng. Anal. Bound. Elements, 26, 639-651.
2. Balas, J., Sladek, J., Sladek, V., 1989, Stress Analysis by Boundary Element Method, Elsevier, Amsterdam.
3. Dong, C.Y., Cheung, Y.K., Lo, S.H., 2002, An Integral Equation Approach to the Inclusion-Crack Interactions in Three-Dimensional Infinite Elastic Domain, Comp. Mech., 29, 313-321.
4. Hirose, S., 1991, Boundary Integral Equation Method for Transient Analysis of 3-D Cavities and Inclusions, Eng. Anal. Bound. Elements, 8, 146-154.
5. Kitahara, M., Nakagawa, K., Achenbach, J.D., 1989, Boundary-Integral Equation Method for Elastodynamic Scattering by a Compact Inhomogeneity, Comp. Mech., 5, 129-144.
6. Shodja, H.M., Rad, I.Z., Soheilifard, R., 2003, Interacting Cracks and Ellipsoidal Inhomogeneities by the Equivalent Inclusion Method, J. Mech. Phys. Solids, 51, 945-960.
7. Sladek, J., Sladek, V., Mykhas'kiv, V.V., Stankevych, V.Z., 2003, Application of Mapping Theory to Boundary Integral Formulation of 3D Dynamic Crack Problems, Eng. Anal. Bound. Elements, 27, 203-213.
8. Xiao, Z.M., Lim, M.K., Liew, K.M., 1994, Stress Intensity Factor of an Elliptical Crack as Influenced by a Spherical Inhomogeneity, Theor. Appl. Fract. Mech., 21, 219-232.
9. Zhang, Ch., Gross, D., 1998, On Wave Propagation in Elastic Solids with Cracks, Comp. Mech. Publ., Southampton.

ZALEŻNOŚĆ POMIĘDZY POWSTAJĄCĄ SZCZELINĄ KOŁOWĄ A SFERYCZNYM TRÓJWYMIAROWYM WTRĄCENIEM W KOMPOZYTACH CZĄSTECZKOWYCH: OBLICZENIA DYNAMICZNEGO WSPÓŁCZYNNIKA INTENSYWNOŚCI NAPRĘŻENIA TYPU-I Z WYKORZYSTANIEM BIEM

Streszczenie

Tematem niniejszej pracy jest analiza zależności pomiędzy powstającą szczeliną kołową a sferycznym sprężystym wtrąceniem osadzonym w nieskończonej sprężystej osnowie, która poddana jest harmonicznemu obciążeniu w płaszczyźnie pękania. Metoda brzegowych równań całkowych (BIEs) została zastosowana do numerycznego rozwiązania problemu w dziedzinie częstotliwości. Eliminacja osobliwości i techniki mapowania są połączone ze schematem kolokacji i zaimplementowane w celu regularyzacji i dyskretyzacji całkowych równań brzegowych poprzez uwzględnienie lokalnej struktury rozwiązania w obszarze wierzchołka pęknięcia. Jako przykład rozważono pęknięcie pojawiające się w warunkach rozciągania ze stałą amplitudą. W tym przypadku środek cząstki leży w płaszczyźnie pęknięcia. Własności wzmacniające wynikające z obecności wtrącenia ujawniają się poprzez dynamiczny współczynnik intensywności naprężenia (SIF) typu-I, który jest funkcją kątową współrzędnej frontu pęknięcia dla różnych częstotliwości i kombinacji materiału osnowy i wtrącenia.

Submitted: October 8, 2008
Submitted in a revised form: November 3, 2008
Accepted: December 1, 2008